2017

Nanosecond Pulsed Electric Field Induced Changes in Cell Surface Charge Density

Diganta Dutta

Xavier-Lewis Palmer
Old Dominion University, xpalm001@odu.edu

Anthony Asmar
Old Dominion University

Michael Stacey
Old Dominion University, mstacey@odu.edu

Shizhi Qian
Old Dominion University, sqian@odu.edu

Original Publication Citation

Dutta, D., Palmer, X.-L., Asmar, A., Stacey, M., & Qian, S. (2017). Nanosecond pulsed electric field induced changes in cell surface charge density. *Micron, 100*, 45-49. doi:10.1016/j.micron.2017.04.009

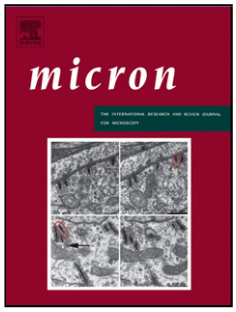

Title: Nanosecond Pulsed Electric Field Induced Changes in Cell Surface Charge Density

Author: Diganta Dutta Xavier-Lewis Palmer Anthony Asmar Michael Stacey Shizhi Qian

PII: S0968-4328(17)30132-4
DOI: http://dx.doi.org/doi:10.1016/j.micron.2017.04.009
Reference: JMIC 2428

To appear in: *Micron*

Received date: 30-3-2017
Revised date: 25-4-2017
Accepted date: 25-4-2017

Please cite this article as: Dutta, D., Palmer, X.-L., Asmar, A., Stacey, M., Qian, S.,Nanosecond Pulsed Electric Field Induced Changes in Cell Surface Charge Density, *Micron* (2017), http://dx.doi.org/10.1016/j.micron.2017.04.009

Nanosecond Pulsed Electric Field Induced Changes in Cell Surface Charge Density

Diganta Dutta[1], Xavier-Lewis Palmer[2], Anthony Asmar[3],

Michael Stacey[3], & Shizhi Qian[4]

[1] Physics and Astronomy, University of Nebraska, Kearney, NE, USA

[2] Biomedical Engineering Institute, Old Dominion University, Norfolk, VA, USA

[3] Frank Reidy Research Center for Bioelectrics, Old Dominion University, Norfolk, VA, USA

[4] Institute of Micro & Nanotechnology, Mechanical & Aerospace Engineering Department, Old Dominion University, Norfolk, VA, USA

Keywords: Atomic Force Microscopy, Jurkat Cell, Surface Charge Density

Abstract

This study reports that the surface charge density changes in Jurkat cells with the application of single 60 nanosecond pulse electric fields, using atomic force microscopy. Using an atomic force microscope tip and Jurkat cells on silica in a 0.01M KCl ionic concentration, we were able to measure the interfacial forces, while also predicting surface charge densities of both Jurkat cell and silica surfaces. The most important finding is that the pulsing conditions varyingly reduced the cells' surface charge density. This offers a novel way in which to examine cellular effects of pulsed electric fields that may lead to the identification of unique mechanical responses. Compared to a single low field strength NsPEF (15 kV/cm) application, exposure of Jurkat cells to a single high field strength NsPEF (60 kV/cm) resulted in a further reduction in charge density and major morphological changes. Both the structure, physics, and chemical

properties of biological cells immensely influence their electrostatic force; we were able to investigate this through the use of atomic force microscopy by measuring the surface forces between the AFM's tip and the Jurkat cells under different pulsing conditions and also the interfacial forces in ionic concentrations.

1. Introduction

The biological effects of pulsed electric fields on cells are of growing interest, and it is well reported that pulses that last longer than the membrane charging time can electroporate the cell membrane. The effects of electroporation can be temporary and beneficial, but this relies on properly monitoring the electric field strength, the number of pulses, and the duration of each pulse (Neumann and Rosenheck, 1972; Shoenbach et al., 2001). Normally, the pulses do not last more than 100 μs, and sub-kV/cm voltages are used, allowing for non-lethal, but large heterogeneous pores to form in the plasma membrane (Gabriel and Teissie, 1999; Gowrishankar and Weaver, 2006; Tekle et al., 1990).

Pulse durations on the scale of nanoseconds are shorter than the charging time of the cell membrane and trigger varying biological effects (Beebe, 2015). Nanosecond pulsed electric fields (NsPEF) create nanopores within the plasma membrane and organelle membranes, disrupting the cytoskeleton and causing externalization of phosphotidylserine proteins (Shoenbach et al., 2001; Beebe, 2015; Pakhomov et al.,2009; Aguiló-Aguayo et al 2008). Thus, it is very apparent that significant membrane events occur, following application of pulsed electric fields that could be measured by changes in membrane surface charge.

The atomic force microscope can quantitate surface charge density, with high spatial resolution, through the sensitivity of its probe tip due to electrostatic interactions (Binning et al 1986). The data from multiple groups provide a consensus among AFM measurements of hard surfaces concerning surface charge density, pH, electrolyte concentration, and coupled Debye Lengths (Ducker et al., 1992; Ducker et al., 1994; Butt et al 2005). Charges from silicon nitride surfaces and various biological membranes have been imaged through double-layer-based contact scanning based on height differentials (Ducker et al., 1992, 1994; Butt et al., 2005). The above results demonstrate the significant qualitative contributions of electrostatics to AFM image contrasting. Further contact mode and topographic scanning are necessary for follow-up quantitative analysis.

In this study, we hypothesized that NsPEF will result in changes to surface charge density due to disruption of the normal surface bioelectrochemistry. Following exposure of cells to NsPEF, we observed an increase in surface charge density that was dependent upon pulsing conditions, suggesting that surface charge may be a means of measuring cellular interaction with electric fields.

2. Methods

2.1 Silica Sample Preparation

A large silica wafer from Montco Silicon Technologies (San Jose, CA, USA) was used to produce the sample surfaces after being cut into 1 cm by 1 cm squares, followed by sonication with 1 M KOH for approximately 15 minutes (Acros Organics, New Jersey, USA). Samples

were then rinsed with deionized water for at least 2 minutes and sonicated with acetone for 15 minutes. The samples were then sonicated in isopropanol (Fisher Scientific Education, Pittsburg, PA, USA) for 15 minutes, before being rinsed with isopropanol and deionized water for at least 2 minutes. Samples were then dried with an air gun and placed on a heating plate for 3 minutes at 120^{o} C. They were then kept in clean boxes to protect against dust deposition prior to experimentation.

2.2 Cell Culture

Cell culturing was followed as in the prior work, Dutta et al 2015 (Dutta et al., 2015). Jurkat E6-1 clones from ATCC were cultured in RPMI 1620 media from Atlanta Biologicals with 10% FBS, 2 mM L-glutamine, 50 IU/mL penicillin, and 50 mg/mL streptomycin (Gibco) at 12 ^{o}C and 5% CO_2 in a humidified incubator. Cultures were maintained within T75 flasks and fresh medium was added every 2-3 days, when cells reached a density of ~3 × 10^6 cells/ml. Cell resuspension was at 1 x 105 g following suspension centrifugation at 200 × g for 5 min.

2.3 Pulsed electric field exposures.

NsPEF exposures utilized a blumline system as was extensively reported (Frey et al., 2006) and calibrated using growth media prior to cellular exposure. Jurkat cells were placed in curvettes (Biosmith, Vandergrift, PA) with 1 mm gaps and then exposed to one 60-nanosecond pulse with field strengths of 0, 15, and 60 kV/cm. The Jurkat cells were immediately fixed, post-exposure, with 4% paraformaldehyde and then were transferred to poly-L-lysine coated

coverslips (Sigma-Aldrich, St. Louis, MO) before being washed in PBS and imaged through AFM.

2.4 Atomic Force Microscopy

We used a Multiview-200 multiple probe AFM from Nanonics Imaging to obtain height, phase, and Near Field Scanning Optical Microscopy images. NWS and WSxM 5.0 imaging and processing software were used respectively for interfacing with the fixed cells on the AFM stage through the use of a 20 nm parabolic quartz tip in tapping mode (Stacey et al., 2013). The tapping mode involves a cantilever oscillation that allows for soft characterizations as the AFM scans (Whited and Park, 2014; Zweyer et al., 2008). The cantilever's spring constant was 800 µN/um, with a resonance frequency of 33.97 kHz. Image calibration was performed using a standard silicon grid and was further verified with a profilometer. Silicon and polydimethylsiloxane (PDMS) were used to process and verify the force measurements.

We used a force separation curve to determine the local molecular forces of the biological cells under hydration with AFM. Interaction forces between the duration of the AFM tip approaching, contacting, and retreating from a given sample are recorded in terms of the force by distance. This process can be exploited to yield many properties as they relate to the mechanical, chemical, electrical, and biological properties of the cell. Furthermore, this task caters well to AFM in that is useful for sensitive work to the level of picoNewtons (Cai et al., 2009; Hsiao et al., 2008)

2.5 Surface Charge Density Mapping

We investigated the electrostatic force of samples in aqueous media since water can charge surfaces through dissociating surface groups or by the surface adsorption of ions, which causes an electric field to decrease exponentially as the surface distance is increased (Mclaughlin, 1977). This occurs even without the presence of free electric charges on the AFM tip, due to electrostatic interaction from polarization charges at the tip-electrolyte interface. Changes in osmotic pressure that occur on the tip and that can contribute to tip repulsion as the surface charges attract counter-ions and trigger ionic concentration increases near the sample need to be considered. The electrostatic force encountered is represented by the equation below, (Parsegian and Gingell, 1977).

$$F_{EDL} = \frac{2\pi R\lambda_D}{\varepsilon\varepsilon_0}\left[2\sigma_s\sigma_t e^{-x/\lambda_D} + (\sigma_s^2 + \sigma_t^2)e^{-2x/\lambda_D}\right] \quad (1)$$

R is the AFM tip radius, ε is the dielectric constant of the medium, ε_0 is the vacuum permittivity, σ_s is the surface charge density of sample, σ_t is the surface charge density of tip, and λ_D is the Debye length, which can be written in the following equation

$$\lambda_D = \sqrt{\frac{\varepsilon\varepsilon_0 k_B T}{2ce^2}} \quad (2)$$

k_B is the Boltzmann constant, T is the temperature, c is the concentration, and e are the charges.

An algorithm, based on the least square fitting method, was developed to measure the biological cells charge density; it was verified with Matlab's CFtool, and both gave similar results. The experimental data was fitted with equation 1 using our code. Equation 1 has two fitting parameters; one is the AFM probe charge density, and the second is the surface charge density. A students t-test was used to show statistical significance.

3. Results

NsPEFs are known to significantly alter cell membrane properties and this phenomenon has been extensively studied computationally and experimentally with regards to pore formation, membrane elasticity, and morphological changes (Gowrishankar and Weaver, 2006; Pakhomov et al., 2009; Aguiló-Aguayo et al., 2008; Frey et al., 2006; Zweyer et al., 2008, Dutta et al., 2015). However, changes in the surface charge of cells, post-exposure to high energy/ low duration electrical fields, is not well documented.

3.1 AFM measurement of charge density

We tested the applicability of the electrostatic force theory with force-distance curves as used by AFM. To do this we developed our own code to fit the theory and experimentally tested this through measurements of the surface force between the AFM tip and the control silica surface within a 0.01 M KCl solution. In tests, our experimental data fit well with theoretical expectations via equation 1 as shown in figure 1a. From these results, the Debye length was independently computed with the use of equation 2. During the AFM probe's approach to the silica surface through all electrical pulsing conditions, continuously increasing repulsive forces

were constantly observed which were found to be a result of similarly charged particles meeting and counter-ion osmotic pressure. At 0 kV/cm, as shown in figure 2a, measurable forces occurred as far as 20 nm from the surfaces of the cells while the tip was able to interact with the cell from as far as 5 nm away, reaching a magnitude of 6.5 nN upon touching the surface of the cells. The surface charge density of Jurkat cells at 0 kV/cm in 0.01 M KCl solution was -0.00852 (±0.00671) C/cm^2. At 15kV/cm (figure 3a), the tip was able to interact with the cell from as far as 4 nm away, reaching a magnitude of 4.3 nN upon touching the cell surfaces. The surface charge density of Jurkat cells at 15 kV/cm in 0.01 M KCl solution was measurably more positive compared to unexposed cells at -0.00159 (±0.00195) C/cm^2. The field strength of 60 kV/cm (figure 4a) allowed the tip to interact with the cell at 3 nm, reaching a magnitude of 2 nN upon touching the cell surfaces and with a further measurable increase in positive value at +0.00176 (±0.00043) C/cm^2. As seen in figures 3a and 4a, the surface charge density of the cells was changed when exposed to a field strength of 15 kV/cm, and this change was even more noticeable with exposure to a field strength of 60 kV/cm. This showed that very high electrical pulsing conditions contributed to an environment in which hydrophilic and hydrophobic cell properties decreased when exposed to low pulsing. In contrast, the unexposed control showed only hydrophobic properties of the cells.

Figure 5 shows three experimental curves fitted and in good agreement with their theoretical pairs. In each curve pairing, the magnitude is decreased with an increasing pulsing condition as ionic concentration decreased above the cellular surfaces. Through biochemical measurements where 0 kV/cm functioned as a control, an 81% decrease in the charge density was found when Jurkat cells were exposed to a field strength of 15 kV/cm (Figure 6); with an even larger change

of 125% decrease of the charge density at surface force measurements through the application of a 60 kV/cm field strength NsPEF (Figure 6). From the data of each experiemental condition, a significant change in charge density due to nanopore formation can be seen through a separation distance decrease and an increase in the force magnitude. The result at 15 kV/cm yielded a significance at $p<0.001$ while the result at 60 kV/cm yielded a significance at $p<0.0001$. The standard deviations and mean value shown in table 1 show respective changes of -0.00159 (±0.0019) for 15 kV/cm and 0.00176 (±0.0004) for 60 kV/cm versus -0.00852 (±0.0067) at 0 kV/cm. These results show significant variations in the cell surface charge under different pulsing conditions.

4. Discussion

This study shows the measurement of nanosecond pulsed electric field effects on surface charge density measurements, and is the first of its kind. We explored how NsPEFs influence cellular surface charge density, through the use of AFM. We performed surface force measurements, on cells and standard silica surfaces, and the results from experimental curves probing the separation of forces over distance were well within the agreement with the electrical double layer theory.

The AFM was our main investigational tool due to its ability to simultaneously acquire local surface and interaction force property measurements, allowing us to determine that cells have a large negatively charged surface density that changed following exposure to NsPEFs. We have previously shown that the AFM has a powerful ability to detect mechanical changes, and now we show the ability of AFM to detect bioelectrochemical changes.

Typically, the effects on the cell membrane are reduced as the pulse duration decreases due to pulses being shorter than the cell membrane charging time. Cell membrane effects, however, are still described following NsPEF, including nanopore formation and externalization of the protein phosphatidylserine (Pakhomov et al., 2009; Beebe, 2015; Vernier et al., 2004), effects that are not thermally induced. The fact that NsPEFs can directly affect protein structure was demonstrated by inactivation of the catalytic activity of the cAMP-dependent protein kinase whose function is highly dependent on structure. (Beebe, 2015; Frey et al., 2006; Pakhomov et al., 2009; Beebe et al., 2004). Similar to our results, greater effects were seen at 60kV/cm compared to 20kV/cm. Other examples of NsPEF induced changes to protein structure can be found although effects are dependent upon pulsing conditions (Aguiló-Aguayo et al., 2008; Li et al., 2007; Xu et al., 1996). Importantly changes in protein structure may expose different charged moieties that can be measured at the cell surface. Plasma membrane voltage changes induced by NsPEF in Jurkat cells (Frey et al., 2006) showed differences dependent upon the orientation of the cell to the electric field, with greater effects at the side facing the cathode. Further work is warranted using our device to more fully characterize differential charge events that are likely dependent upon the orientation of the cell to the NsPEF (Pakhomov et al., 2009). Future work involves investigating the electrical energy measurements of the cells under differing NsPEF regimes.

In conclusion, our data demonstrates that NsPEFs significantly can change cell membrane surface charge densities. Under both NsPEF regimes, surface charge density increased, but this occurred more so with the high field strengths. Our experimental data may potentially help the development of nanomedicine for cancer and other disease therapies. This goes especially for

therapies relying on novel exploitation of cell surface properties and the nanoenvironment surrounding the cells.

Acknowledgements

Research reported in this publication was supported by the National Institute of Arthritis and Musculoskeletal and Skin Diseases of the National Institute of Health under the award number R17AR063254. The content is solely the responsibility of the authors and does not necessarily represent the views of the NIH.

References

Aguiló-Aguayo, I., Odriozola-Serrano, I., Quintão-Teixeira, L.J., Martín-Belloso, O., 2008. Inactivation of tomato juice peroxidase by high-intensity pulsed electric fields as affected by process conditions. Food Chemistry 107, 949–955. http://dx.doi.org/10.1016/j.foodchem.2007.08.057

Beebe, S.J., Blackmore, P.F., White, J., Joshi, R.P., Schoenbach, K.H., 2004. Nanosecond pulsed electric fields modulate cell function through intracellular signal transduction mechanisms. Physiological Measurement 25, 1077–1093. http://dx.doi.org/10.1088/0967-3334/25/4/023

Beebe, S.J., 2015. Considering effects of nanosecond pulsed electric fields on proteins. Bioelectrochemistry 103, 52–59. https://doi.org/10.1016/j.bioelechem.2014.08.014

Binnig, G., Quate, C.F., Gerber, C., 1986. Atomic Force Microscope. Physical Review Letters 56, 930–933. https://doi.org/10.1103/PhysRevLett.56.930

Butt, H.-J.C.B.C., Cappella, B., Kappl, M., 2005. Force measurements with the atomic force microscope: Technique, interpretation and applications. Surface Science Reports 59, 1 152. http://dx.doi.org/10.1016/j.surfrep.2005.08.003

Cai, X., Gao, S., Cai, J., Wu, Y., Deng, H., 2009. Artesunate induced morphological and mechanical changes of Jurkat cell studied by AFM. Scanning 31, 83–89. https://doi.org/10.1002/sca.20144

Ducker, W.A., Senden, T.J., Pashley, R.M., 1992. Measurement of forces in liquids using a force microscope. Langmuir 8, 1831–1836. https://doi.org/10.1021/la00043a024

Ducker, W.A., Xu, Z., Israelachvili, J.N., 1994. Measurements of Hydrophobic and DLVO Forces in Bubble-Surface Interactions in Aqueous Solutions. Langmuir 10, 3279–3289. https://doi.org/10.1021/la00021a061

Dutta, D., Asmar, A., Stacey, M., 2015. Effects of nanosecond pulse electric fields on cellular elasticity. Micron 72, 15–20. https://doi.org/10.1016/j.micron.2015.01.004

Frey, W., White, J., Price, R., Blackmore, P., Joshi, R., Nuccitelli, R., Beebe, S., Schoenbach, K., Kolb, J., 2006. Plasma Membrane Voltage Changes during Nanosecond Pulsed Electric Field Exposure. Biophysical Journal 90, 3608–3615. https://doi.org/10.1529/biophysj.105.072777

Gabriel, B., Teissié, J., 1999. Time Courses of Mammalian Cell Electropermeabilization Observed by Millisecond Imaging of Membrane Property Changes during the Pulse. Biophysical Journal 76, 2158–2165. https://doi.org/10.1016/s0006-3495(99)77370-4

Gowrishankar, T., Weaver, J.C., 2006. Electrical behavior and pore accumulation in a multicellular model for conventional and supra-electroporation. Biochemical and Biophysical Research Communications 349, 643–653. https://doi.org/10.1016/j.bbrc.2006.08.097

Hsiao, S.E.C., Crow, A.K., Lam, W.A., Bertozzi, C.R., Fletcher, D.A., Francis, M.B., 2008. DNA- Coated AFM Cantilevers for the Investigation of Cell Adhesion and the Patterning of Live Cells. Angewandte Chemie International Edition 47, 8473–8477. https://doi.org/10.1002/anie.200802525

Li, Y., Chen, Z., Mo, H., 2007. Effects of pulsed electric fields on physicochemical properties of soybean protein isolates. LWT - Food Science and Technology 40, 1167–1175. https://doi.org/10.1016/j.lwt.2006.08.015

Mclaughlin, S., 1977. Electrostatic Potentials at Membrane-Solution Interfaces. Current Topics in Membranes and Transport 71–144. https://doi.org/10.1016/s0070-2161(08)60677-2

Neumann, E., Rosenheck, K., 1972. Permeability changes induced by electric impulses in vesicular membranes. The Journal of Membrane Biology 10, 279–290. https://doi.org/10.1007/bf01867861

Pakhomov, A.G., Bowman, A.M., Ibey, B.L., Andre, F.M., Pakhomova, O.N., Schoenbach, K.H., 2009. Lipid nanopores can form a stable, ion channel-like conduction pathway in cell membrane. Biochemical and Biophysical Research Communications 385, 181–186. https://doi.org/10.1016/j.bbrc.2009.05.035

Parsegian, V., Gingell, D., 1972. On the Electrostatic Interaction across a Salt Solution between Two Bodies Bearing Unequal Charges. Biophysical Journal 12, 1192–1204. https://doi.org/10.1016/s0006-3495(72)86155-1

Schoenbach, K.H., Beebe, S.J., Buescher, E.S., 2001. Intracellular effect of ultrashort electrical pulses. Bioelectromagnetics 22, 440–448. https://doi.org/10.1002/bem.71

Stacey, M., Dutta, D., Cao, W., Asmar, A., Elsayed-Ali, H., Kelly, R., Beskok, A., 2013. Atomic force microscopy characterization of collagen 'nanostraws' in human costal cartilage. Micron 44, 483–487. https://doi.org/10.1016/j.micron.2012.10.006

Tekle, E., Astumian, R.D., Chock, P.B., 1990. Electro-permeabilization of cell membranes: Effect of the resting membrane potential. Biochemical and Biophysical Research Communications 172, 282–287. https://doi.org/10.1016/s0006-291x(05)80206-2

Vernier, P.T., Sun, Y., Marcu, L., Craft, C.M., Gundersen, M.A., 2004. Nanoelectropulse-Induced Phosphatidylserine Translocation. Biophysical Journal 86, 4040–4048. https://doi.org/10.1529/biophysj.103.037945

Whited, A.M., Park, P.S.-H., 2014. Atomic force microscopy: A multifaceted tool to study membrane proteins and their interactions with ligands. Biochimica et Biophysica Acta (BBA) - Biomembranes 1838, 56–68. https://doi.org/10.1016/j.bbamem.2013.04.011

Xu, D., Phillips, J.C., Schulten, K., 1996. Protein Response to External Electric Fields: Relaxation, Hysteresis, and Echo. The Journal of Physical Chemistry 100, 12108–12121. https://doi.org/10.1021/jp960076a

Zweyer, M., Troian, B., Spreafico, V., Prato, S., 2008. SNOM on cell thin sections: observation of Jurkat and MDAMB453 cells. Journal of Microscopy 229, 440–446. https://doi.org/10.1111/j.1365-2818.2008.01925.x

Figure 1: Silica surface AFM imaging

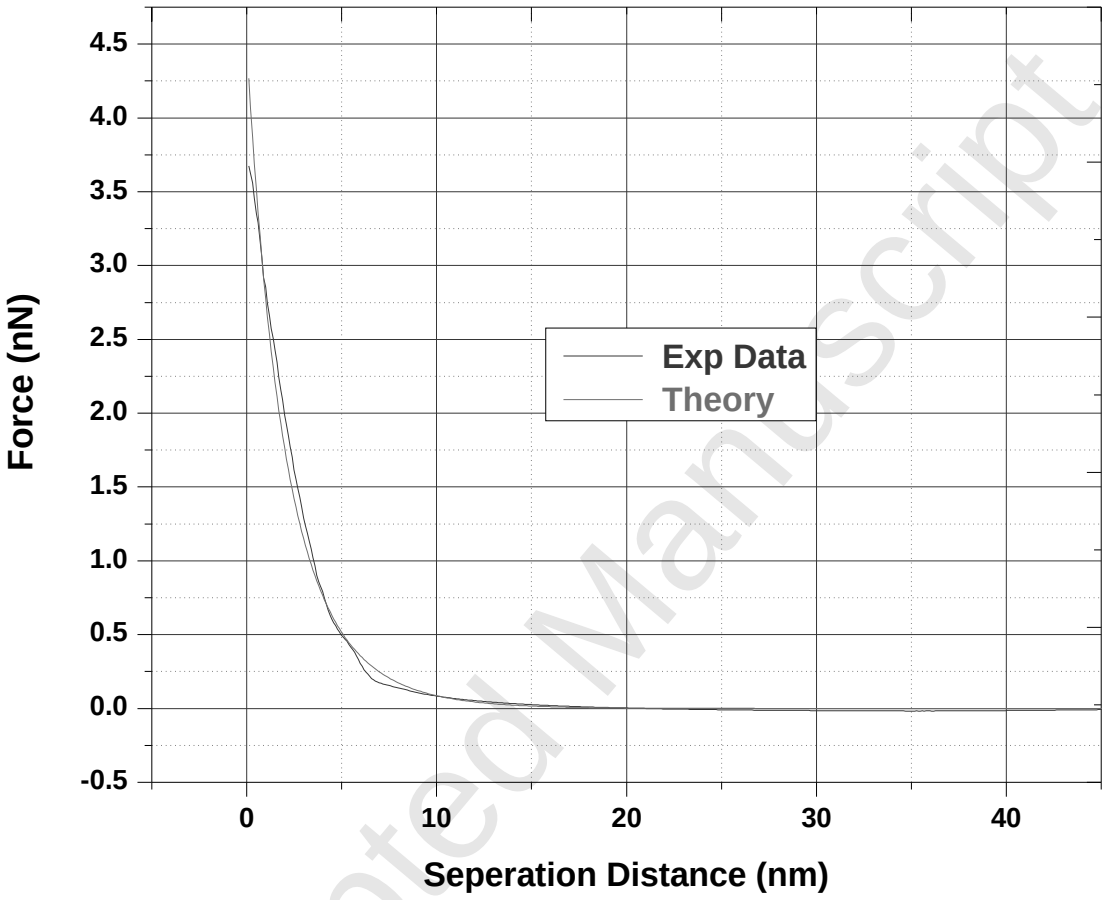

Figure 1a: Surface force measurements between AFM probe and Silica in 0.01 M KCl solution

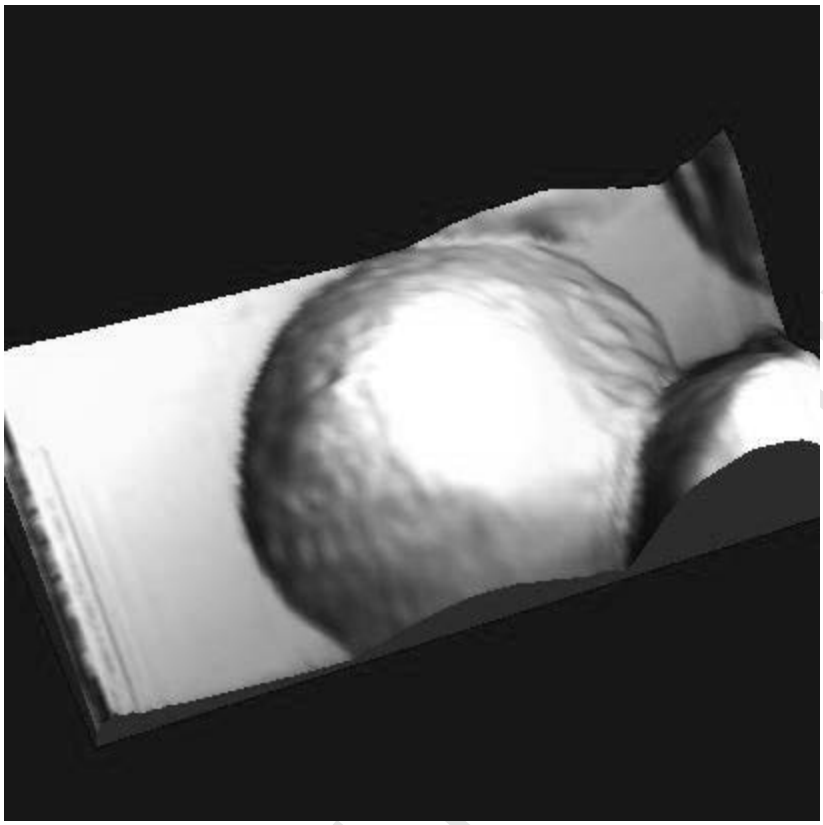

Figure 2: Jurkat Cells (0 kV/cm) AFM imaging

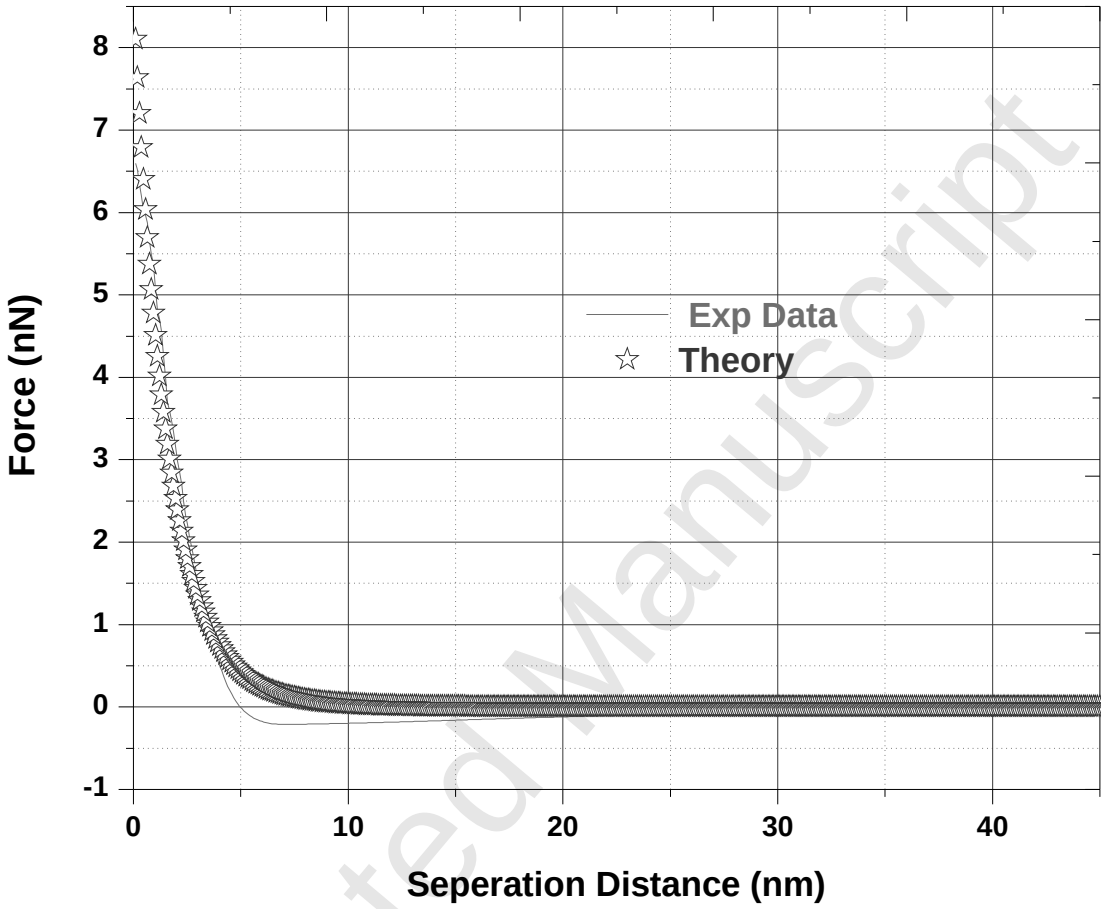

Figure 2a: Surface force measurements between AFM probe and Jurkat Cells (0 kV/cm) in 0.01 M KCl solution

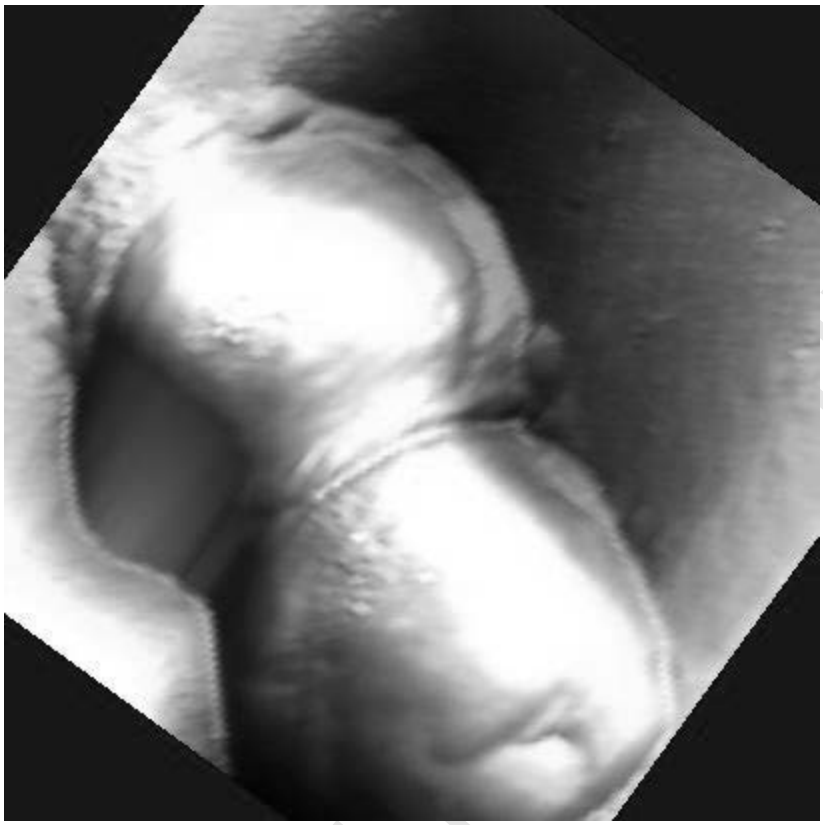

Figure 3: Jurkat Cells (15 kV/cm) AFM imaging

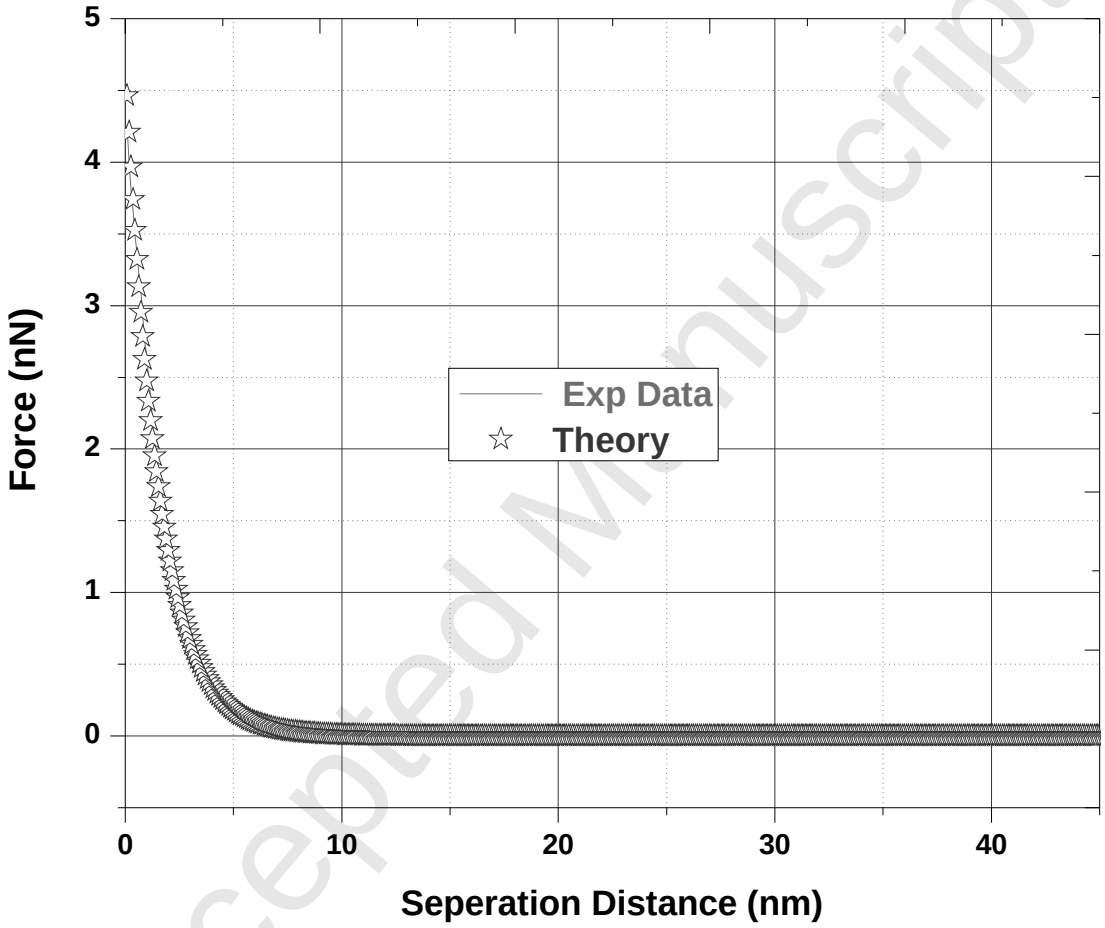

Figure 3a: Surface force measurements between AFM probe and Jurkat Cells (15 kV/cm) in 0.01 M KCl solution

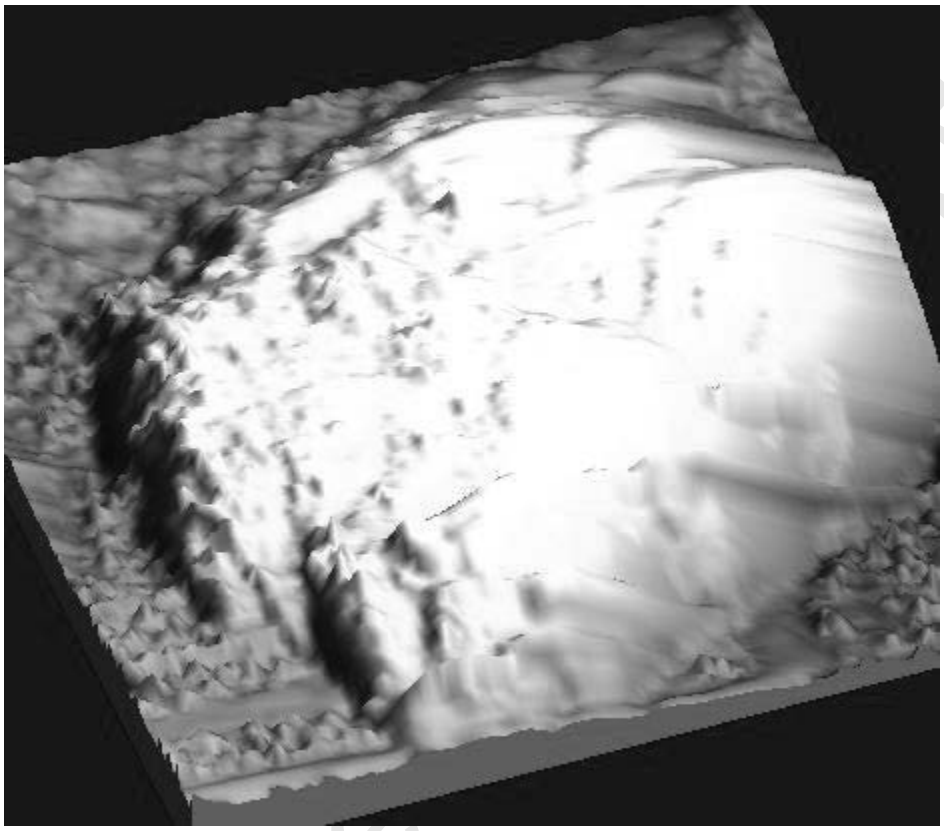

Figure 4: Jurkat Cells (60 kV/cm) AFM imaging

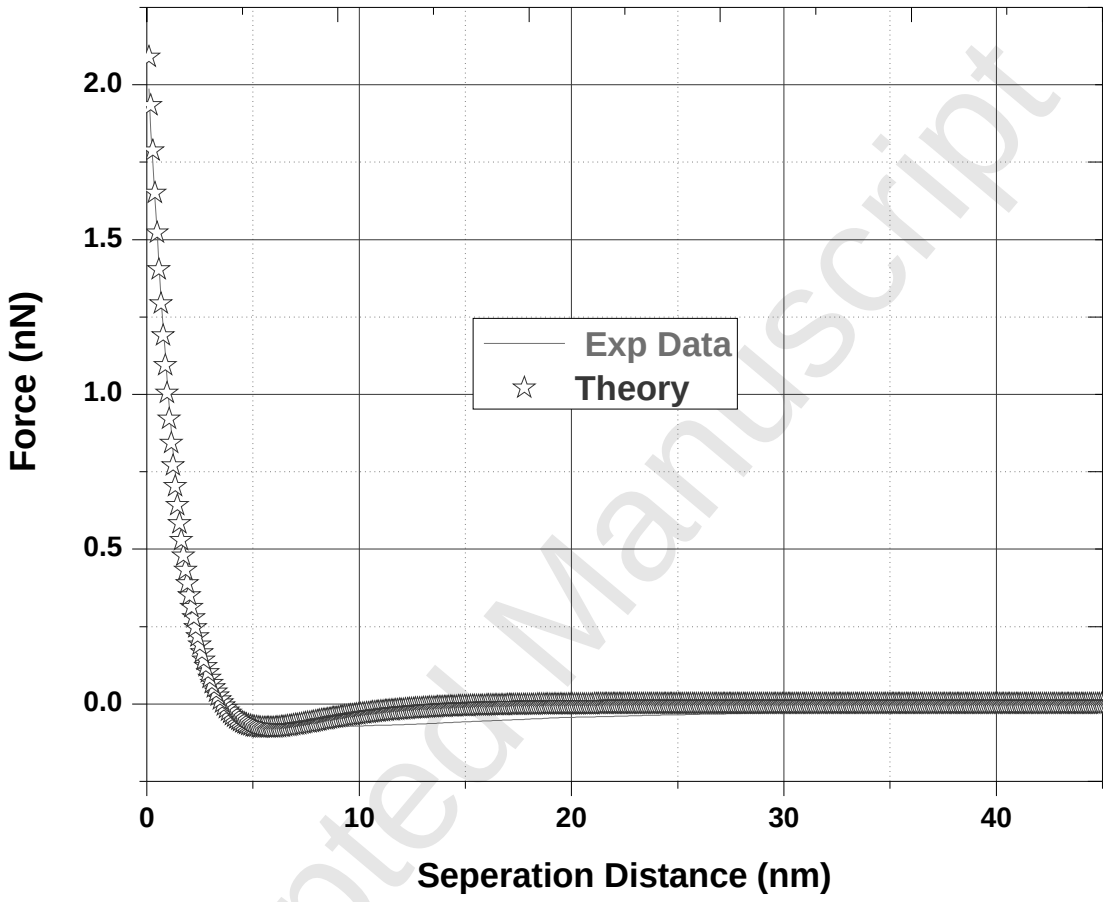

Figure 4a: Surface force measurements between AFM probe and Jurkat Cells (60kV/cm) in 0.01 M KCl solution

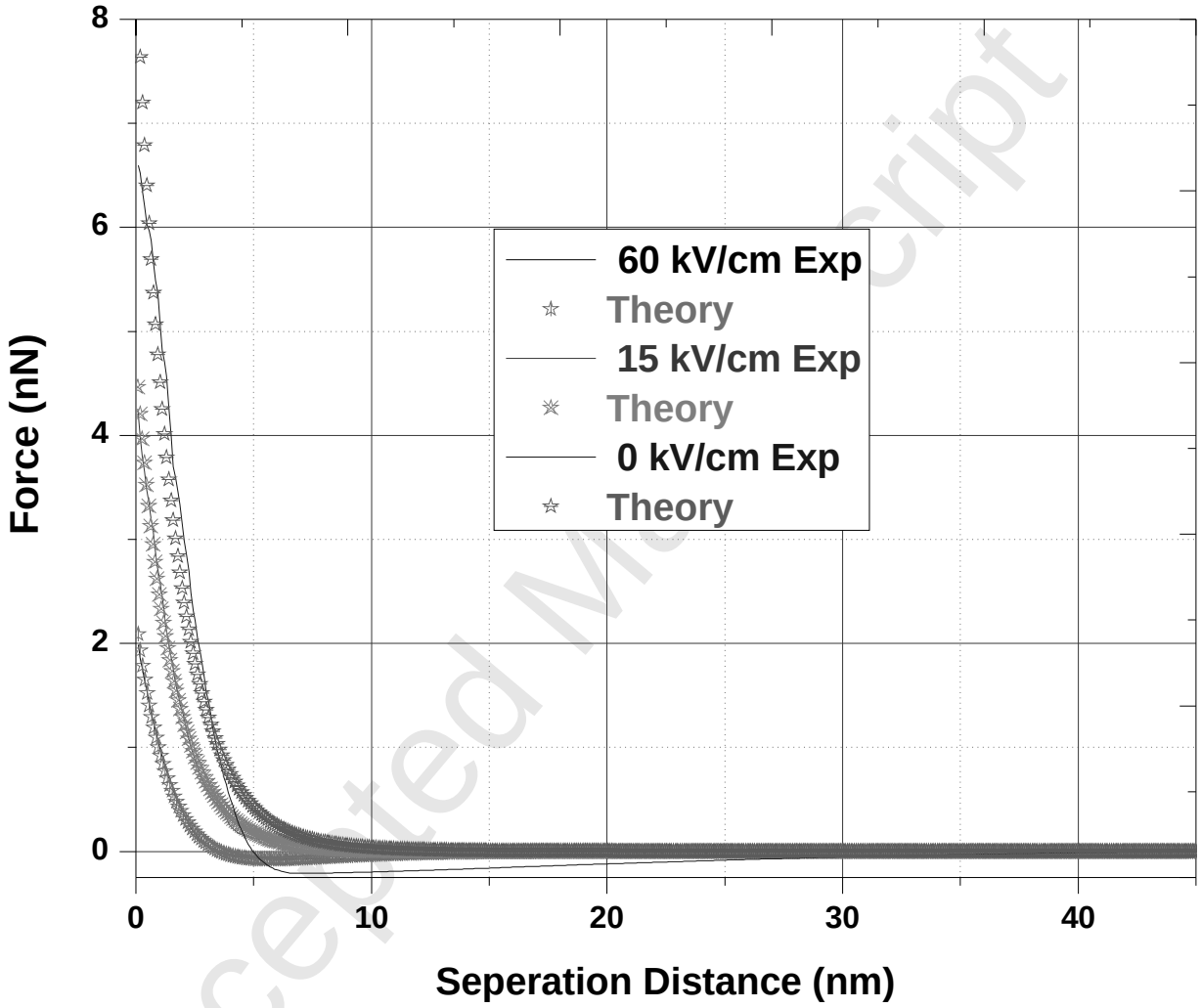

Figure 5: Comparison of all 3 surface force measurements between AFM probe and Jurkat Cells

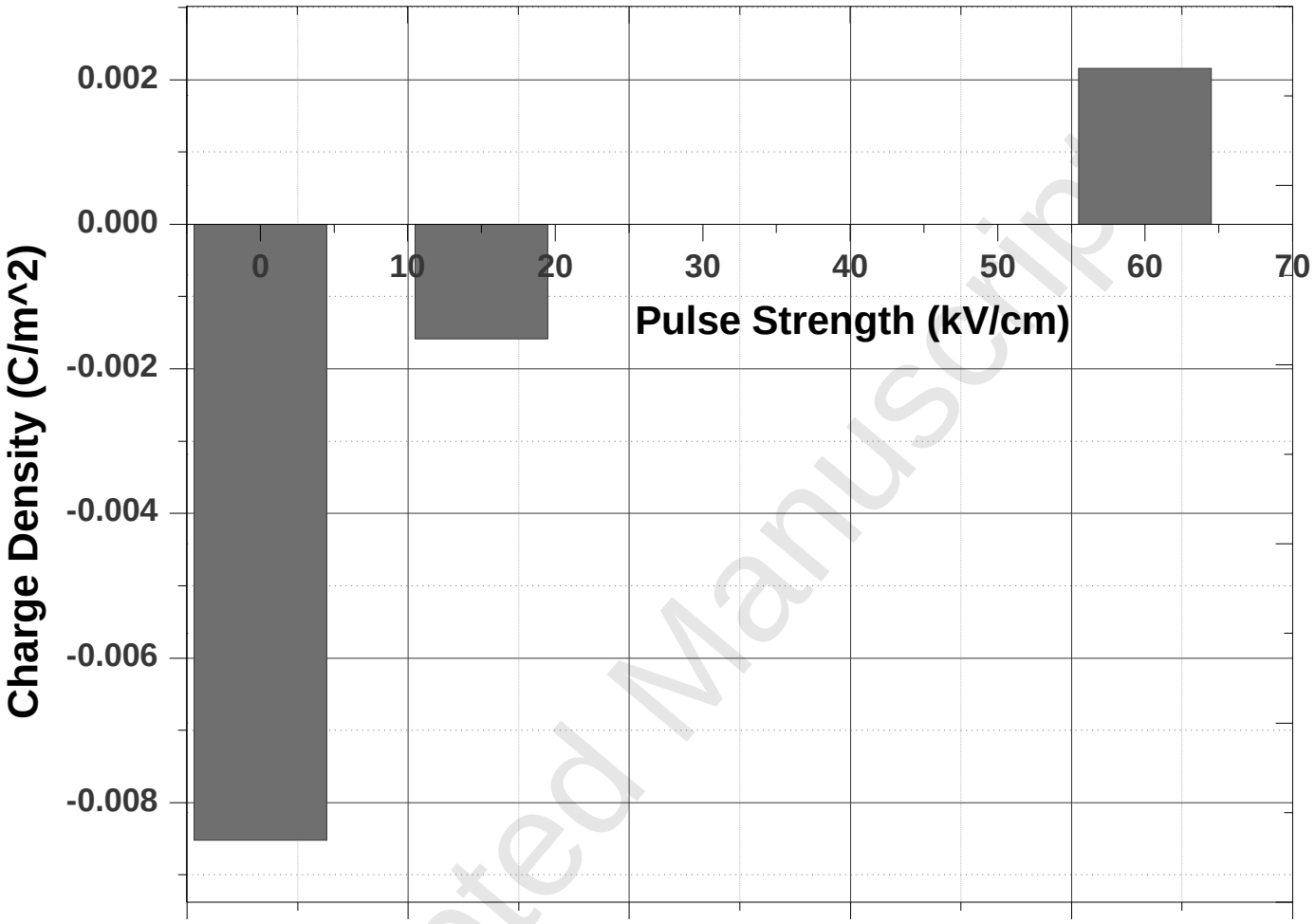

Figure 6: Surface charge density measurements in cells pulsed for 60 ns at 0, 15, and 60 kV/cm

(n = 3 for all conditions)

Cells Surface Charge Density

Conditions	0 kV/cm	15 kV/cm	60 kV/cm
Average (SD)	-0.00852 (±0.0067)	-0.00159 (±0.0019)	0.00176 (±0.0004)
% of reduction from 0 kV/cm	-	81%**	125%***

Calculated charge density in C/cm^2

** Statistically significant ($p<0.001$)

*** Statistically significant ($p<0.0001$)